Published in final edited form as:
Microvasc Res. 2010 December ; 80(3): 295–302. doi:10.1016/j.mvr.2010.05.011.

Improved assessment of laser-induced choroidal neovascularization

Hassanain S. Toma[a], **Joshua M. Barnett**[b], **John S. Penn**[a,b], and **Stephen J. Kim**[a,*]

[a]Department of Ophthalmology and Visual Sciences, Vanderbilt University Medical Center, Nashville, TN, USA

[b]Department of Pharmacology, Vanderbilt University School of Medicine, Nashville, TN, USA

Abstract

The primary objective of this study was to develop and evaluate new methods of analyzing laser-induced choroidal neovascularization (CNV), in order to make recommendations for improving the reporting of experimental CNV in the literature. Six laser burns of sufficient power to rupture Bruch's membrane were concentrically placed in each eye of 18 adult Norway rats. Eyes received intravitreal injections of either triamcinolone acetonide, ketorolac, or balanced salt solution (BSS). Fluorescein angiography (FA) was performed 2 and 3 weeks after injection, followed by choroidal flat mount preparation. Vascular leakage on FAs and vascular budding on choroidal mounts were quantified by measuring either the cross-sectional area of each CNV lesion contained within the best-fitting polygon using Adobe Photoshop (Lasso Technique or Quick Selection Technique), or the area of bright pixels within a lesion using Image-Pro Plus. On choroidal mounts, the Lasso Technique and Image-Pro Plus detected a significant difference in lesion size between either ketorolac or triamcinolone when compared to BSS, while the Quick Selection Technique did not (Lasso Technique, 0.78 and 0.64; Image-Pro Plus, 0.77 and 0.65). On FA, the Lasso Technique and Quick Selection Technique detected a significant difference in lesion size between either ketorolac or triamcinolone when compared to BSS, while Image-Pro Plus did not (Lasso Tool, 0.81 and 0.54; Quick Selection Tool, 0.76 and 0.57). Choroidal mounts and FA are both valuable for imaging experimental CNV. Adobe Photoshop and Image-Pro Plus are both able to detect subtle differences in CNV lesion size, when images are not manipulated. The combination of choroidal mounts and FA provides a more comprehensive assessment of CNV anatomy and physiology.

Keywords

Age-related macular degeneration; AMD; Choroidal neovascularization; CNV; Laser-induced CNV

Introduction

Choroidal neovascularization (CNV) is the most common cause of severe vision loss in patients with age-related macular degeneration (AMD) and is responsible for substantial vision loss in pathologic myopia (Soubrane, 2008), presumed ocular histoplasmosis

*Corresponding author. Vanderbilt Eye Institute, 2311 Pierce Avenue, Nashville, TN, 37232, USA. Fax: +1 615 936 1540., skim30@gmail.com (S.J. Kim).

Conflict of interest statement
No conflicting relationship exists for any author.

syndrome (Prasad and Van Gelder, 2005), angioid streaks (Clarkson and Altman, 1982), and idiopathic polypoidal choroidal vasculopathy (Yannuzzi et al., 1990). In all of these conditions, CNV results from the growth of new blood vessels into the subretinal space through a break in Bruch's membrane. The laser-induced animal model, whether employed on mice, rats, rabbits, or monkeys, is arguably the most established and commonly utilized model worldwide for studying the pathogenesis of CNV and its response to treatment (Dobi et al., 1989; Tobe et al., 1998).

The most frequently employed technique to image and quantify laser-induced CNV lesions is achieved by preparing and dissecting choroidal tissue (choroidal mounting), staining for neovascular blood vessel growth, imaging the lesions with a camera, and performing two dimensional measurements of the CNV lesions. Fluorescein angiography (FA) is another well-established technique used to evaluate ocular neovascularization, which requires the injection of sodium fluorescein followed by visualizing its flow within the vasculature using a fundus camera. However, FAs are commonly restricted to large animals and human applications.

Nonetheless, in the literature, numerous and wide ranging methods have been utilized to measure CNV on choroidal mounts and FA (Campa et al., 2008; Campos et al., 2006; Chakravarthy et al., 2007; Criswell et al., 2008; Edelman and Castro, 2000; Narasimha-Iyer et al., 2006; Sickenberg et al., 1999). However, results vary considerably depending on which technique is used to quantify the CNV lesions, making it difficult to compare results among the above referenced studies. For instance, some methods are unable to detect small, but significant, changes in CNV lesions due to their subjective and categorical nature, such as classifying lesions as mild, moderate, severe or based on the presence or absence of leakage (Dobi et al., 1989; Husain et al., 1999; Kanai et al., 2000; Nishiwaki et al., 2002; Obana et al., 2000; Qu et al., 2009; Tobe et al., 1998; Wang et al., 2007; Zacks et al., 2002). Therefore, the purpose of this study is to develop new and compare existing methods of analyzing laser-induced CNV, on both choroidal mounts and FAs, to determine their validity and reliability in order to make recommendations that may improve the consistency of CNV reporting.

Materials and methods

All procedures were performed with strict adherence to guidelines for animal use and experimentation of the Vanderbilt University Animal Care and Use Committee, and the Association for Research in Vision and Ophthalmology.

Animals and Treatments

Eighteen Brown-Norway male rats (Charles River Laboratories, Inc; Wilmington, Massachusetts) were evaluated in this study. Anesthesia for laser photocoagulation, examination, and photography was performed by intramuscular injection of ketamine hydrochloride, 50 mg/kg and xylazine hydrochloride, 5 mg/kg. Topical proparacaine (0.5%) was applied for corneal anesthesia. Tropicamide (1%) and phenylephrine hydrochloride (2.5%) were applied for pupillary dilation.

We have previously reported that treatment of laser-induced CNV with triamcinolone acetonide (Kenalog-40, Bristol-Myers Squibb; Princeton, NJ), dramatically reduces CNV formation and ketorolac (Sigma; St. Louis, MO) moderatively reduces CNV formation when compared to balanced salt solution (BSS, Alcon; FortWorth, TX; Kimand Toma, 2010). Therefore, to test our techniques' accuracy in distinguishing different CNV sizes, each of these was intravitreally injected in a group of six rats immediately after laser photocoagulation.

Laser photocoagulation

Animals were positioned before a slit lamp (Carl Zeiss Meditec, Inc; Jena, Germany) laser delivery system. The fundus was visualized using a microscope slide cover slip with 2.5% hydroxypropyl methylcellulose solution as an optical coupling agent. An argon green laser (Coherent, Polo Alto; CA, USA) was used for photocoagulation (532 nm wavelength; 360 mW power; 0.07-s duration; and 50 μm spot size). This setting most reliably produced acute vapor bubbles, indicative of the rupture of Bruch's membrane. In each eye, six focal laser photocoagulation lesions were concentrically applied approximately two optic discs from the center, while avoiding major blood vessels. Immediately after laser treatment, animals were divided into three groups (triamcinolone, ketorolac, BSS) for intravitreal injections. A total of 72 lesions (12 eyes) were present for each treatment group. No eyes were excluded due to lens trauma or severe vitreous bleeding. Laser rupture sites which had subretinal bleeding at the time of lasering were excluded from analysis and represented less than 10% of total rupture sites in each treatment group.

Intravitreal injections

Prior to and immediately following injection, topical Vigamox (moxifloxacin HCI ophthalmic solution 0.5%, Alcon; Fort Worth, TX) was applied. Under stereomicroscopic guidance, a 30-gauge needle with a 19° bevel and a 10-μl syringe (Hamilton Co.; Reno, NV) was used to penetrate the superior sclera just posterior to the ora serrata, and a volume of 5 μl of either triamcinolone (40 mg/ml), ketorolac dissolved in BSS (30 mg/ml), or BSS was injected into the vitreous cavity. Both eyes of each animal received the same treatment to avoid the possibility of a crossover effect. A total of six animals (12 eyes) were injected per treatment group. None of the rats met the exclusion criteria, which included cataract, vitreous hemorrhage, or death.

Fluorescein angiography

At 2 and 3 weeks after intravitreal injection, all animals underwent fluorescein angiography (FA) using a digital fundus camera (Carl Zeiss Meditec, Inc) with a viewing angle set at 50 degrees. For a wider viewing angle a 20 diopter lens was placed in front of the fundus camera's viewing lens. For fluorescein angiographic evaluations, 0.3 ml of 10% sodium fluorescein was administered intraperitoneally, and photographs were taken at predesignated times (30 s, 1, 2, 5, 10 and 15 min). Five minute (±1 min) phase angiograms were found to be optimal and most consistent with mid phase, and used for all comparative analyses.

Choroidal mounts and tissue staining

Choroidal mounts and tissue staining were performed in a manner similar to that described by Bora et al. (2005). In brief, animals were euthanized by cervical dislocation immediately after 3-week FA imaging. The eyes were then enucleated and stored in 10% formalin for 2 h. The retinal pigment epithelium (RPE)-choroid- sclera flat mounts were obtained by hemisecting the eyes, removing the lens, and peeling the neural retina away from the underlying RPE. At least four radial cuts were made to allow the tissue to be flattened. Endothelial cells of CNV were identified with FITC-conjugated isolectin B4 (Sigma; St. Louis, MO) while the elastin of the extracellular matrix was identified using goat anti-elastin antibody conjugated to Cy3 (Santa Cruz Biotech., Inc; Santa Cruz, CA). The eyecup was then placed flat with the RPE-side facing up onto a microscope slide. Gel Mount media (Biomedia; Victoria, Australia) was applied to the tissue before covering the tissue with a cover slip.

Choroidal mounts were visualized using the 10× objective of an epifluorescent compound microscope fitted with the appropriate excitation and emission filters (Provis AX-70,

Olympus; Japan). Images of the neovascular lesions were captured using a digital camera attached to the Provis system (DP71, Olympus; Japan) coupled to a PC with image capture software (DP Controller, Olympus; Japan). Image sizes were calibrated using the DP Controller's built-in scale bar feature.

Analysis of CNV on choroidal mounts

The extent of CNV vascular budding at each rupture site on choroidal mounts was determined by measuring the pixel area within the circumference of each lesion using three different methods. All measurements were performed at 100% image magnification. All images were unaltered, except where noted. Pixel area was identified from the image histogram set at a cache level 1.

For the first method (Fig. 1A), the pixel area of vascular budding was traced by a trained, masked investigator using the “lasso” selection tool (Lasso Technique) in Adobe Photoshop CS3 (Adobe Systems Inc.; San Jose, CA). The cross-sectional area of each CNV lesion was quantified as the area contained within the best-fitting polygon. Although this method is subjective in nature, we felt that it constituted the best standard technique of reference to evaluate CNV lesions on choroidal mounts since it is a preferred method to measure CNV in the animal model of laser-induced CNV (Edelman and Castro, 2000).

For the second method, color images were converted to black and white by using the “levels” option in Adobe Photoshop CS3 to select the area under the image histogram, ranging from 90% (lower limit) to 95% (upper limit). Images were uniformly modified this way in order to create sharply contrasting lesion border, which was necessary for detection by the “quick selection tool” (Fig. 1B). This tool (Quick Selection Technique), set at a diameter of 50 pixels and hardness of 0%, was then continuously applied by a masked investigator until the selection area of vascular budding ceased to expand beyond the lesion, as dictated by the software's built-in edge detection algorithm. The area of each CNV lesion was quantified as the area contained within the best-fitting polygon. These parameters were empirically chosen to best emulate lesion selection by the Lasso Technique.

For the third method, vascular budding were measured using Image-Pro Plus software (Image-Pro Plus 6.0, Media Cybernetics; Silver Spring, MD). A masked investigator manually traced an area containing the lesion using the “area of interest” tool. The Image-Pro Plus default algorithm for automatically measuring bright objects, was then applied to measure the pixel area (the brightly stained endothelial cells) contained within the areas of vascular budding (Fig. 1C).

Analysis of CNV on fluorescein angiograms

The extent of CNV staining and leakage at each lesion site on FA was similarly determined by measuring the area within the circumference of each lesion using the Lasso Technique, Quick Selection Technique, and Image-Pro Plus. The Lasso Technique was applied exactly as described for choroidal mounts with tracing of CNV lesions performed by a trained, masked retina specialist (Fig. 1D). This method constitutes the best standard technique of reference to evaluate CNV lesions on FAs, since measurement of lesion area by trained specialists has been shown to be consistent and reliable, as demonstrated in the Wisconsin age-related maculopathy grading system (Klein et al., 1991, 1992; Mitchell et al., 1995; Tan et al., 2008).

Unlike choroidal mounts, FAs are naturally captured in grayscale, and hence, the Quick Selection Techniques was applied without the need for image modification (Fig. 1E).

The background microvasculature on FA images made it difficult for Image-Pro Plus to identify lesion area, and for this reason images were converted to black and white using an intensity cutoff value of 205; pixels darker or brighter than an intensity value of 205 were turned black or white, respectively. To further separate CNV area from the surrounding microvasculature, the Image-Pro Plus "erosion" filter was applied, with the filter parameters set at "2 × 2 boxes" and "5 passes." This resulted in the complete attrition of the background microvasculature, and to a lesser extent, the lesion as well. The "dilatation" filter, set at "2 × 2 boxes" and "5 passes," was then applied in an attempt to negate the effects of the "erosion" filter on the CNV lesion. The Image-Pro Plus default algorithm for automatically measuring bright objects was then employed to measure CNV pixel area (Fig. 1F). These parameters were empirically chosen to best emulate lesion selection by the Lasso Technique.

Relative ratios

The mean pixel area of CNV in the ketorolac and triamcinolone injected eyes was divided by that of BSS injected eyes to obtain a relative ratio. Relative ratios were calculated for each method because they automatically adjust for large differences in pixel area that existed between choroidal mounting and FA. For example, the average pixel area of CNV for choroidal mounts ranged from 200,000 to 300,000, but only 5000 to 9000 on FA due to differences in image magnification. Thus, relative ratios enable direct comparison between choroidal mounts and FA.

Statistics

Descriptive statistics including mean±95% confidence interval (CI) were calculated for continuous characteristics. The D'Agostino-Pearson normality test confirmed that the data was distributed normally. Each treatment group (triamcinolone or ketorolac) was compared to control (BSS) using a two-tailed unpaired t-test with unequal variance. A $p<0.05$ was considered statistically significant. Statistical significance between relative ratios was determined using mean and CI.

Results

CNV lesions on choroidal mounts

Representative images of CNV vascular budding on choroidal mounts 3 weeks after intravitreal injection are shown in Fig. 2A, B, and C. As expected, by visual inspection, eyes injected with triamcinolone have reduced vascular budding compared to BSS injected eyes. Ketorolac injected eyes also show reduced vascular budding, but to a lesser degree than triamcinolone.

As mentioned earlier, the Lasso Technique was set as the standard technique of reference. The Lasso Technique and Image-Pro Plus detected a significant difference ($p<0.05$) in mean CNV vascular budding between ketorolac and triamcinolone injected eyes (Fig. 3). In addition, both the Lasso Technique and Image-Pro Plus also detected a significant difference ($p<0.05$) in vascular budding in ketorolac (210 ± 12 μm^2 and 168 ± 9 μm^2, respectively) and triamcinolone (188 ± 13 μm^2 and 155 ± 8 μm^2, respectively) injected eyes when compared to BSS eyes (235 ± 14 μm^2 and 190 ± 10 μm^2, respectively). However, in contrast to the Lasso Technique, the Quick Selection Technique failed to detect a significant difference in vascular budding in the ketorolac (152 ± 9 μm^2) or triamcinolone (164 ± 10 μm^2) injected eyes when compared to BSS (156 ± 9 μm^2).

The relative ratio for ketorolac and triamcinolone injected eyes was 0.78 and 0.64, respectively, using the Lasso Technique, 0.96 and 1.09, respectively, using the Quick Selection Technique, and 0.77 and 0.65, respectively, using Image Pro-Plus (Fig. 4A).

Relative ratios obtained for ketorolac and triamcinolone injected eyes were almost identical for the Lasso Technique and Image-Pro Plus, indicating a CNV reduction of 22–23% for ketorolac and 35–36% for triamcinolone (Fig. 4B). However, the Quick Selection Technique showed a reduction of only 4% for ketorolac and an actual increase of 9% for triamcinolone.

CNV lesions on fluorescein angiograms

Representative images of CNV lesions on FA at 2 and 3 weeks after intravitreal injection are shown in Fig. 5A, B, and C. As in the case of choroidal mounts, eyes injected with triamcinolone qualitatively demonstrate a reduction in CNV staining and leakage compared to BSS injected eyes. Ketorolac injected eyes also show reduced staining and leakage, but to a lesser degree than triamcinolone.

As mentioned earlier, the Lasso Technique was set as the standard technique of reference. At 2 (Fig. 6A) and three (Fig. 6B) weeks after injection, the Lasso Technique detected significantly ($p<0.05$) less CNV staining and leakage on FA in both ketorolac (7789 ± 783 and 8782 ± 725 at 2 and 3 weeks, respectively) and triamcinolone (5197 ± 451 and 6767 ± 878, respectively) injected eyes than BSS (9628 ± 1205 and 9852 ± 697, respectively) injected eyes. At both 2 and 3 weeks, the Lasso Technique also detected a significant difference ($p<0.05$) in staining and leakage between ketorolac and triamcinolone injected eyes.

At 2 and 3 weeks, the Quick Selection Technique similarly detected significantly ($p<0.05$) less CNV staining and leakage in both ketorolac (7390 ± 972 and 8349 ± 1022, respectively) and triamcinolone (5536 ± 323 and 6647 ± 710, respectively) injected eyes than BSS (9750 ± 1669 and 10463 ± 1141, respectively) injected eyes (Fig. 6A and B). At both 2 and 3 weeks, the Quick Selection Technique detected a significant difference ($p<0.05$) in staining and leakage between ketorolac and triamcinolone injected eyes.

In contrast to both the Lasso and Quick Selection Techniques, Image-Pro Plus (Fig. 6A and B) detected significantly less ($p<0.05$) CNV staining and leakage in triamcinolone injected eyes at 2 and 3 weeks (6165 ± 2065 and 8941 ± 2472, respectively), but not ketorolac injected eyes (12057 ± 1875 and 10981 ± 1831, respectively) when compared to BSS injected eyes (13529 ± 2110 and 13383 ± 2221, respectively). Furthermore, Image-Pro Plus only detected a significant difference ($p<0.05$) in CNV staining and leakage between ketorolac and triamcinolone injected eyes at 2, but not at 3, weeks.

Relative ratios for ketorolac and triamcinolone injected eyes on FA at 2 weeks was 0.81 and 0.54, respectively, using the Lasso Technique, 0.76 and 0.57, respectively, using the Quick Selection Technique, and 0.89 and 0.46, respectively, using Image Pro-Plus (Fig. 7). Relative ratios for ketorolac and triamcinolone injected eyes on FA at 3 weeks was 0.89 and 0.69, respectively, using the Lasso Technique, 0.80 and 0.64, respectively, using the Quick Selection Technique, and 0.82 and 0.67, respectively, using Image Pro-Plus (Fig. 8).

Discussion

CNV occurs in only 10% of all AMD cases, but is responsible for approximately 90% of all blindness (Ferris et al., 1984). By the year 2050, the number of people aged 65 years and older in the United States will more than double to 82.7 million (Rein et al., 2009) and the number of Americans aged 80 years and older is expected to grow to nearly 35 million. Since the prevalence of CNV in AMD increases dramatically with age, the prevalence of CNV is also expected to proportionally increase. For this reason, understanding the physiology and pathogenesis of CNV in order to develop new treatments remains an urgent priority.

In this regard, laser induction of CNV is arguably the most commonly used model worldwide to study the pathogenesis of CNV and its response to treatment. Although a senescent AMD mouse model has recently been introduced (Ambati et al., 2003; Chan et al., 2008; Hollyfield et al., 2008), CNV occurs in a relatively small percentage of eyes and at randomtimes and locations making this model ill suited for interventional studies. Nevertheless, the methods of analysis, detailed herein, should also be readily applicable to the genetic and other mouse models. Despite the importance of laser induction as a model to study AMD, there is no uniformly accepted method to analyze or report CNV. This is problematic as different imaging techniques and methods of analysis make direct comparison among studies impossible and results difficult to interpret. Furthermore, absence of accepted standards of reporting allows for selection bias, since methods of varying accuracy may be chosen preferentially.

Consequently, the purpose of this study was to systematically compare and contrast the two most established CNV imaging techniques, choroidal mounting and FA, to determine their degree of correlation. In addition, we rigorously compared and contrasted three different methods of analyzing laser-induced CNV in the setting of three different CNV lesion sizes resulting from three pharmacologic treatments. The results of our study indicate that while both FA and choroidal mounts are capable of distinguishing subtle differences in CNV lesion size, FA may offer some advantages because it can be used to assess vascular competency and allows for longitudinal studies in animals.

Although FA has been used clinically for nearly half a century (Dollery et al., 1962; Norton et al., 1965; Novotny and Alvis, 1961), choroidal tissue mounting is the most commonly used technique to evaluate CNV in animal models today. Nevertheless, FA offers several advantages over choroidal tissue mounting as it provides real-time images of CNV lesions, allows for assessment of blood vessel integrity, and most importantly enables serial measurements for longitudinal evaluation in individual eyes. To our knowledge, this is the first direct comparison of choroidal mounting and FA with respect to their ability to distinguish differences in CNV lesion size. Although we observed good correlation between the two techniques, we consistently observed greater inhibitory effects on CNV with triamcinolone using FA, as reflected by smaller relative ratios. This is not surprising since choroidal mounting only measures anatomical area of vascular budding, while FA measures the combination of anatomical area and pathological leakage.

In addition, FA allows for serial measurements, which strengthens the reliability of results as more than one time point is available for comparison. The neovascular plexus in choroidal mounts has been shown to reach its maximal size and density by day 10 with no significant increase in size thereafter to 31 days (Edelman and Castro, 2000). The reproducibility of the Lasso, Quick Selection, and Image-Pro Plus techniques was further assessed by comparing CNV lesions on FA at 2 and 3 weeks after treatment. In this study, we found excellent reproducibility of CNV measurement with less than 3%, 7%, and 1% variance for the Lasso, Quick Selection, and Image-Pro Plus techniques, respectively. These data support the reliability of FA and demonstrate its potential to improve reporting of CNV when used alone or in concert with choroidal mounting.

Although FA is the “gold standard” for assessing CNV in human clinical trials (1996; Arias et al., 2008; Essex et al., 2003; Mann et al., 2008), it is used less frequently in animal studies, due in part to poor rates of visualizing CNV on FA in earlier reports (Dobi et al., 1989). However, our experience and recent reports (Lu and Adelman, 2009) demonstrate that the success rate of CNV detection on FA has dramatically improved over time owing to refinements of the technique. In this study approximately 95% of the laser-induced lesions produced CNV.

In cases where FA is used, however, there is substantial variation in CNV reporting. Recently published methods include describing CNV staining on FA relative to the size of optic nerve head (Sickenberg et al., 1999), by measuring diameter of CNV lesion along an axis (Criswell et al., 2008), by assessing lesion size based on the presence or absence of leakage (Dobi et al., 1989; Husain et al., 1999; Kanai et al., 2000; Obana et al., 2000; Tobe et al., 1998; Zacks et al., 2002), by using a qualitative grading method (Nishiwaki et al., 2002; Qu et al., 2009;Wang et al., 2007), and by measuring the CNV staining perimeter using imaging software (Funakoshi et al., 2006). None of these methods have been validated and many of them are arguably unable to detect small, but significant, changes in CNV lesion size due to their subjective and categorical (mild, moderate, severe) nature. Moreover, many of these methods are difficult to precisely replicate and thus, ill suited to recommend for general adoption. Furthermore, our techniques all provide quantified measurements of the entire CNV lesion area, regardless of shape. This characteristic is essential, in our opinion, as many CNV lesions are irregularly shaped and thus, measuring axial length or circumference alone, as reported by others (Criswell et al., 2008; Funakoshi et al., 2006) appears inherently less accurate.

To establish more standardized methods of reporting CNV, we analyzed digital FA images using widely and commercially available imaging software (Adobe Photoshop and Image-Pro Plus) and used parameters and modifications that could be consistently replicated by others. The Lasso Technique, using the “Lasso” tool in Adobe Photoshop, represented a completely subjective method since it relied entirely on identification and tracing of CNV lesion area by a masked, trained investigator. The Quick Selection Technique using the “Quick Selection” Tool on Adobe Photoshop relied on subjective and objective elements. It required a masked investigator to identify and trace the area of CNV by continuous application of the “Quick Selection” tool, as deemed necessary, to completely cover the area of interest. Each application of the tool increased the traced area by a pre-set amount determined by relative brightness. The Image-Pro Plus technique, on the other hand, represented a more objective method since it did not depend on a masked grader to trace lesion area, but instead relied on the software's own default algorithm for measurement. All three methods consistently distinguished three different CNV lesion sizes created by treatment with intravitreal triamcinolone, ketorolac, or BSS.

Although Image-Pro Plus compared favorably to our standard technique of reference in detecting CNV budding on choroidal mounts, it failed to do so when employed on FA. Its detection of CNV staining and leakage using FA was more variable, as reflected by the larger confidence intervals for each of the treatment groups (Fig. 6A and B). Consequently, it failed to detect a statistically significant difference in CNV lesion size between ketorolac and BSS injected groups at both 2 and 3 weeks, and between triamcinolone and ketorolac at 3 weeks, in contrast to both the Lasso and Quick Selection Techniques. We believe that image conversion to black and white (binary image) and application of erosion and dilation filters, which were necessary to reduce background vasculature, resulted in a loss of the relatively dim spectrum of pixels that make up a portion of CNV. This is a drawback of setting an artificial intensity cutoff value to create binary images. This loss of pixels appeared to negatively affect the reliability and sensitivity of Image-Pro Plus. Thus, while all three methods showed comparable trends, we discourage the use of filters and arbitrary cutoff values to create binary images for this reason.

Although the Quick Selection Technique was proficient at quantifying CNV on FA, it did not accurately detect differences in CNV area on choroidal mounts. While both the Lasso Technique and Image-Pro Plus correlated well and demonstrated a significant decrease in CNV vascular budding of 22% and 23%, respectively, for ketorolac and 36% and 35%, respectively, for triamcinolone injected eyes, the Quick Selection Technique demonstrated a

decrease of only 4% for ketorolac and an actual increase of 9% for triamcinolone. The "quick selection" tool is the only automated tracing tool in Adobe Photoshop that selects objects based on their relative, rather than absolute brightness. This feature reduced the potential of over detecting or under detecting relatively well circumscribed CNV lesions on FA images due to variation in brightness. However, CNV lesions on choroidal mounts typically have irregular borders due to peripheral vascular budding with patchy fluorescence (Fig. 1A). Despite conversion of images to black and white (Fig. 1B), the Quick Selection Technique was unable to accurately detect these irregular borders and thus, underestimated lesion area in eyes treated with BSS, and to a lesser extent ketorolac, where greater vascular budding was present. Furthermore, the use of binary images may have resulted in the loss of relatively dim pixels, as previously discussed, which would have minimized differences between CNV lesions. These factors combined were likely responsible for the failure of the Quick Selection Technique to detect significant differences between the three treatment groups.

As with all studies, our results should be interpreted with caution. An important underlying premise of our study was that treatment with triamcinolone and ketorolac would have different inhibitory effects on CNV. Although it is well established that triamcinolone is a potent inhibitor of CNV (Ciulla et al., 2001; Falkenstein et al., 2008; Kato et al., 2005; Tatar et al., 2009), ketorolac's inhibitory effect has only been recently established (Kim and Toma, 2010).

However, several other studies have reported inhibition of CNV with other nonsteroidal anti-inflammatory drugs (Hu et al., 2005; Takahashi et al., 2003, 2004).

In addition our direct intraocular injection of ketorolac explains its greater inhibitory effect on CNV when compared to previous studies which relied on systemic or topical application (Baranano et al., 2009; Castro et al., 2004). Although the use of isolectin B4 to stain and measure CNV is well established (Lee and Rewolinski, 2009; Yanni et al., 2009), it may have resulted in background staining of the laser rupture site on choroidal mounts which may have resulted in our overestimation of CNV lesion size for both triamcinolone and ketorolac treated eyes. However, we do not believe this had any effect on our conclusions since this was a comparative study which focused on inter-method agreement and not on pharmacologic effect.

In conclusion, the Lasso Technique accurately measures CNV on both choroidal mounts and FA in contrast to the other techniques, which are accurate on one, but not both, imaging methods. Image manipulation techniques, such as the application of erosion or dilatation filter, or setting arbitrary cutoff values to create binary images should be discouraged, as they limit the ability to detect subtle differences between lesions. Furthermore, evaluation of CNV using the combination of choroidal mounts and FAs provides corroboration of results and a more comprehensive assessment of CNV anatomy and physiology and should therefore be encouraged. General application of our results may improve the reporting of experimental CNV.

Acknowledgments

We would like to thank Rueben Banalagay for his technical assistance with Image-Pro Plus.

Supported in part by EY07533 (JSP), AG031036 (JMB), and an Unrestricted Grant from Research to Prevent Blindness.

References

Ambati J, Anand A, Fernandez S, Sakurai E, Lynn BC, Kuziel WA, Rollins BJ, Ambati BK. An animal model of age-related macular degeneration in senescent Ccl-2- or Ccr-2-deficient mice. Nat. Med. 2003; 9:1390–1397. [PubMed: 14566334]

Arias L, Caminal JM, Casas L, Masuet C, Badia MB, Rubio M, Pujol O, Arruga J. A study comparing two protocols of treatment with intravitreal bevacizumab (Avastin) for neovascular age-related macular degeneration. Br. J. Ophthalmol. 2008; 92:1636–1641. [PubMed: 18782803]

Baranano DE, Kim SJ, Edelhauser HF, Durairaj C, Kompella UB, Handa JT. Efficacy and pharmacokinetics of intravitreal non-steroidal anti-inflammatory drugs for intraocular inflammation. Br. J. Ophthalmol. 2009; 93:1387–1390. [PubMed: 19628498]

Bora PS, Sohn JH, Cruz JM, Jha P, Nishihori H, Wang Y, Kaliappan S, Kaplan HJ, Bora NS. Role of complement and complement membrane attack complex in laser-induced choroidal neovascularization. J. Immunol. 2005; 174:491–497. [PubMed: 15611275]

Campa C, Kasman I, Ye W, Lee WP, Fuh G, Ferrara N. Effects of an anti-VEGF-A monoclonal antibody on laser-induced choroidal neovascularization in mice: optimizing methods to quantify vascular changes. Invest. Ophthalmol. Vis. Sci. 2008; 49:1178–1183. [PubMed: 18326747]

Campos M, Amaral J, Becerra SP, Fariss RN. A novel imaging technique for experimental choroidal neovascularization. Invest. Ophthalmol. Vis. Sci. 2006; 47:5163–5170. [PubMed: 17122098]

Castro MR, Lutz D, Edelman JL. Effect of COX inhibitors on VEGF-induced retinal vascular leakage and experimental corneal and choroidal neovascularization. Exp. Eye Res. 2004; 79:275–285. [PubMed: 15325574]

Chakravarthy U, Walsh AC, Muldrew A, Updike PG, Barbour T, Sadda SR. Quantitative fluorescein angiographic analysis of choroidal neovascular membranes: validation and correlation with visual function. Invest.Ophthalmol. Vis. Sci. 2007; 48:349–354. [PubMed: 17197553]

Chan CC, Ross RJ, Shen D, Ding X, Majumdar Z, Bojanowski CM, Zhou M, Salem N Jr, Bonner R, Tuo J. Ccl2/Cx3cr1-deficient mice: an animal model for age-related macular degeneration. Ophthalmic Res. 2008; 40:124–128. [PubMed: 18421225]

Ciulla TA, Criswell MH, Danis RP, Hill TE. Intravitreal triamcinolone acetonide inhibits choroidal neovascularization in a laser-treated rat model. Arch. Ophthalmol. 2001; 119:399–404. [PubMed: 11231773]

Clarkson JG, Altman RD. Angioid streaks. Surv. Ophthalmol. 1982; 26:235–246. [PubMed: 7046115]

Criswell MH, Hu WZ, Steffens TJ, Li R, Margaron P. Comparing pegaptanib and triamcinolone efficacy in the rat choroidal neovascularization model. Arch. Ophthalmol. 2008; 126:946–952. [PubMed: 18625941]

Dobi ET, Puliafito CA, Destro M. A new model of experimental choroidal neovascularization in the rat. Arch. Ophthalmol. 1989; 107:264–269. [PubMed: 2464985]

Dollery CT, Hodge JV, Engel M. Studies of the retinal circulation with flourescein. Br. Med. J. 1962; 2:1210–1215. [PubMed: 14028474]

Edelman JL, Castro MR. Quantitative image analysis of laser-induced choroidal neovascularization in rat. Exp. Eye Res. 2000; 71:523–533. [PubMed: 11040088]

Essex RW, Qureshi SH, Cain MS, Harper CA, Guymer RH. Photodynamic therapy in practice: a review of the results of the first 12 months experience with verteporfin at the Royal Victorian Eye and Ear Hospital. Clin. Exp. Ophthalmol. 2003; 31:476–481.

Falkenstein IA, Cheng L, Wong-Staal F, Tammewar AM, Barron EC, Silva GA, Li QX, Yu D, Hysell M, Liu G, Ke N, Macdonald JE, Freeman WR. Toxicity and intraocular properties of a novel long-acting anti-proliferative and anti-angiogenic compound IMS2186. Curr. Eye Res. 2008; 33:599–609. [PubMed: 18600493]

Ferris FL 3rd, Fine SL, Hyman L. Age-related macular degeneration and blindness due to neovascular maculopathy. Arch. Ophthalmol. 1984; 102:1640–1642. [PubMed: 6208888]

Funakoshi T, Birsner AE, D'Amato RJ. Antiangiogenic effect of oral 2-methoxyestradiol onchoroidal neovascularization inmice. Exp. EyeRes. 2006; 83:1102–1107.

Hollyfield JG, Bonilha VL, Rayborn ME, Yang X, Shadrach KG, Lu L, Ufret RL, Salomon RG, Perez VL. Oxidative damage-induced inflammation initiates age-related macular degeneration. Nat. Med. 2008; 14:194–198. [PubMed: 18223656]

Hu W, Criswell MH, Ottlecz A. Oral administration of lumiracoxib reduces choroidal neovascular membrane development in the rat laser-trauma model. Retina. 2005; 25(8):1054–1064. [PubMed: 16340537]

Husain D, Kramer M, Kenny AG, Michaud N, Flotte TJ, Gragoudas ES, Miller JW. Effects of photodynamic therapy using verteporfin on experimental choroidal neovascularization and normal retina and choroid up to 7 weeks after treatment. Invest. Ophthalmol. Vis. Sci. 1999; 40:2322–2331. [PubMed: 10476799]

Kanai M, Obana A, Gohto Y, Nagata S, Miki T, Kaneda K, Nakajima S. Longterm effectiveness of photodynamic therapy by using a hydrophilic photosensitizer ATX-S10(Na) against experimental choroidal neovascularization in rats. Lasers Surg. Med. 2000; 26:48–57. [PubMed: 10637003]

Kato A, Kimura H, Okabe K, Okabe J, Kunou N, Nozaki M, Ogura Y. Suppression of laser-induced choroidal neovascularization by posterior sub-tenon administration of triamcinolone acetonide. Retina. 2005; 25:503–509. [PubMed: 15933599]

Kim SJ, Toma HS. Inhibition of choroidal neovascularization by intravitreal ketorolac. Arch. Ophthalmol. 2010; 128:596–600. [PubMed: 20457981]

Klein R, Davis MD, Magli YL, Segal P, Klein BE, Hubbard L. The Wisconsin age-related maculopathy grading system. Ophthalmology. 1991; 98:1128–1134. [PubMed: 1843453]

Klein R, Klein BE, Linton KL. Prevalence of age-related maculopathy. The Beaver Dam Eye Study. Ophthalmology. 1992; 99:933–943. [PubMed: 1630784]

Lee ES, Rewolinski D. Evaluation for CXCR4 inhibition in the prevention and intervention model of laser-induced choroidal neovascularization. Invest. Ophthalmol. Vis. Sci. 2009 Electronic publication ahead of print.

Lu F, Adelman RA. Are intravitreal bevacizumab and ranibizumab effective in a rat model of choroidal neovascularization? Graefes Arch. Clin. Exp. Ophthalmol. 2009; 247:171–177. [PubMed: 18781316]

Mann AL, Bressler SB, Hawkins BS, Holekamp N, Bressler NM. Comparison of methods to identify incident cataract in eyes of patients with neovascular maculopathy: Submacular Surgery Trials Report No. 18. Ophthalmology. 2008; 115:127–133. [PubMed: 17574675]

Mitchell P, Smith W, Attebo K, Wang JJ. Prevalence of age-related maculopathy in Australia. The Blue Mountains Eye Study. Ophthalmology. 1995; 102:1450–1460. [PubMed: 9097791]

Narasimha-Iyer H, Can A, Roysam B, Stern J. Automated change analysis from fluorescein angiograms for monitoring wet macular degeneration. Conf. Proc. IEEE Eng. Med. Biol. Soc. 2006; 1:4714–4717. [PubMed: 17947113]

Nishiwaki H, Zeimer R, Goldberg MF, D'Anna SA, Vinores SA, Grebe R. Laser targeted photo-occlusion of rat choroidal neovascularization without collateral damage. Photochem. Photobiol. 2002; 75:149–158. [PubMed: 11883603]

Norton EW, Gass JD, Smith JL, Curtin VT, David NJ, Justice J Jr. Macular diseases: diagnosis. Fluorescein in the study of macular disease. Trans. Am. Acad. Ophthalmol. Otolaryngol. 1965; 69:631–642. [PubMed: 14345768]

Novotny HR, Alvis DL. A method of photographing fluorescence in circulating blood in the human retina. Circulation. 1961; 24:82–86. [PubMed: 13729802]

Obana A, Gohto Y, Kanai M, Nakajima S, Kaneda K, Miki T. Selective photodynamic effects of the new photosensitizer ATX-S10(Na) on choroidal neovascularization in monkeys. Arch. Ophthalmol. 2000; 118:650–658. [PubMed: 10815157]

Prasad AG, Van Gelder RN. Presumed ocular histoplasmosis syndrome. Curr. Opin. Ophthalmol. 2005; 16:364–368. [PubMed: 16264347]

Qu Y, Zhang S, Xu X, Wang H, Li J, Zhou F, Wei F. Octreotide inhibits choroidal neovascularization in rats. Ophthalmic Res. 2009; 42:36–42. [PubMed: 19478539]

Rein DB, Wittenborn JS, Zhang X, Honeycutt AA, Lesesne SB, Saaddine J. Forecasting age-related macular degeneration through the year 2050: the potential impact of new treatments. Arch. Ophthalmol. 2009; 127:533–540. [PubMed: 19365036]

Sickenberg M, Ballini JP, van den Bergh H. A computer-based method to quantify the classic pattern of choroidal neovascularization in order to monitor photodynamic therapy. Graefes Arch. Clin. Exp. Ophthalmol. 1999; 237:353–360. [PubMed: 10333100]

Soubrane G. Choroidal neovascularization in pathologic myopia: recent developments in diagnosis and treatment. Surv. Ophthalmol. 2008; 53:121–138. [PubMed: 18348878]

Takahashi K, Saishin Y, Saishin Y, Mori K, Ando A, Yamamoto S, Oshima Y, Nambu H, Melia MB, Bingaman DP, Compochiaro PA. Topical nepafenac inhibits ocular neovascularization. Invest. Ophthalmol. Vis. Sci. 2003; 44(1):409–415. [PubMed: 12506103]

Takahashi H, Yanagi Y, Tamaki Y, Uchida S, Muranaka K. COX-2-selective inhibitor, etodolac, suppresses choroidal neovascularization in a mice model. Biochem. Biophys. Res. Commun. 2004; 325(2):461–466. [PubMed: 15530415]

Tan JS, Wang JJ, Flood V, Rochtchina E, Smith W, Mitchell P. Dietary antioxidants and the long-term incidence of age-related macular degeneration: the Blue Mountains Eye Study. Ophthalmology. 2008; 115:334–341. [PubMed: 17664009]

Tatar O, Adam A, Shinoda K, Kaiserling E, Boeyden V, Claes C, Eckardt C, Eckert T, Pertile G, Scharioth GB, Yoeruek E, Szurman P, Bartz-Schmidt KU, Grisanti S. Early effects of intravitreal triamcinolone acetonide on inflammation and proliferation in human choroidal neovascularization. Arch. Ophthalmol. 2009; 127:275–281. [PubMed: 19273790]

Tobe T, Ortega S, Luna JD, Ozaki H, Okamoto N, Derevjanik NL, Vinores SA, Basilico C, Campochiaro PA. Targeted disruption of the FGF2 gene does not prevent choroidal neovascularization in a murine model. Am. J. Pathol. 1998; 153:1641–1646. [PubMed: 9811357]

Wang FE, Shi G, Niesman MR, Rewolinski DA, Miller SS. Receptor tyrosine kinase inhibitors AG013764 and AG013711 reduce choroidal neovascularization in rat eye. Exp. Eye Res. 2007; 84:922–933. [PubMed: 17399700]

Yanni SE, Barnett JM, Clark ML, Penn JS. The role of PGE2 receptor EP4 in pathologic ocular angiogenesis. Invest. Ophthalmol. Vis. Sci. 2009; 50:5479–5486. [PubMed: 19494202]

Yannuzzi LA, Sorenson J, Spaide RF, Lipson B. Idiopathic polypoidal choroidal vasculopathy (IPCV). Retina. 1990; 10:1–8. [PubMed: 1693009]

Zacks DN, Ezra E, Terada Y, Michaud N, Connolly E, Gragoudas ES, Miller JW. Verteporfin photodynamic therapy in the rat model of choroidal neovascularization: angiographic and histologic characterization. Invest.Ophthalmol. Vis. Sci. 2002; 43:2384–2391. [PubMed: 12091441]

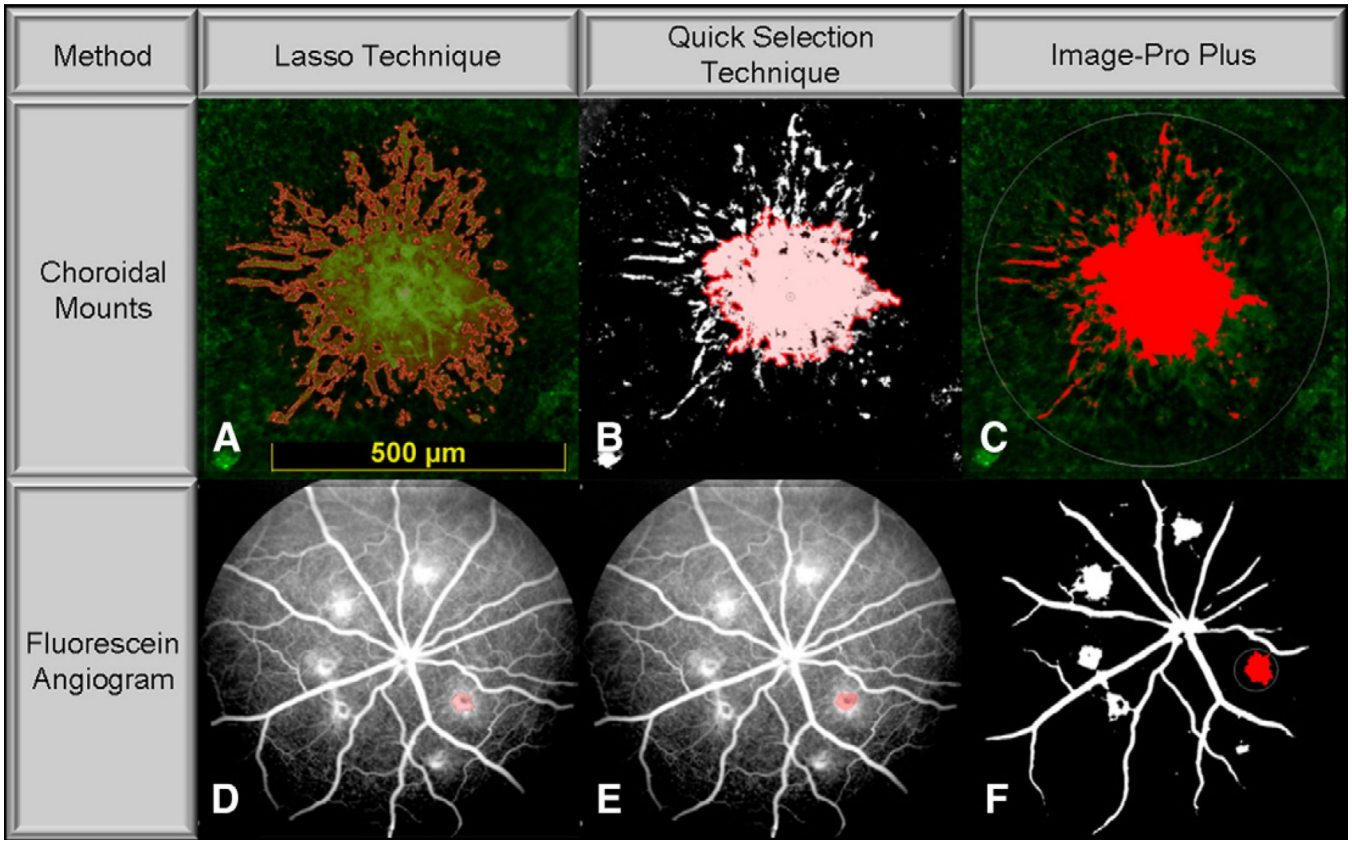

Fig. 1.
Illustrative images of different techniques. Illustrative images of laser-induced choroidal neovascularization (CNV) on choroidal mounts and fluorescein angiograms (FA) demonstrating application of the Lasso Technique (A and D); Quick Selection Technique (B and E); and Image-Pro Plus (C and F).

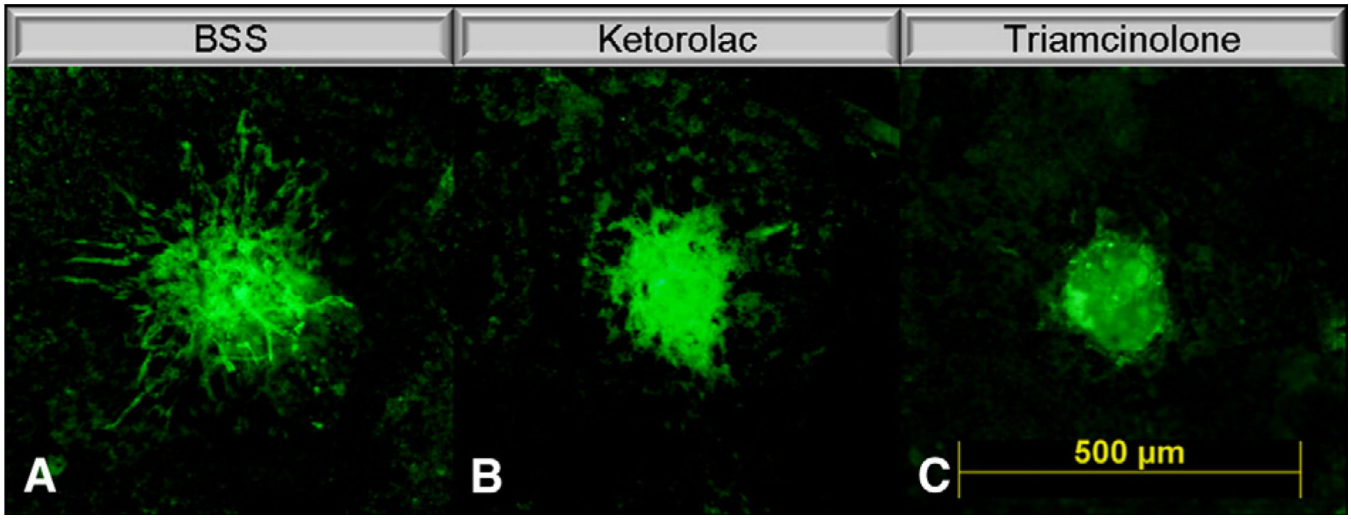

Fig. 2.

Laser-induced CNV on choroidal mounts. Representative images of laser-induced (CNV) 3 weeks after injection of (A) balanced salt solution (BSS), (B) ketorolac, or (C) triamcinolone. Note dramatically reduced vascular budding in triamcinolone and to a lesser extent ketorolac injected eyes compared to BSS.

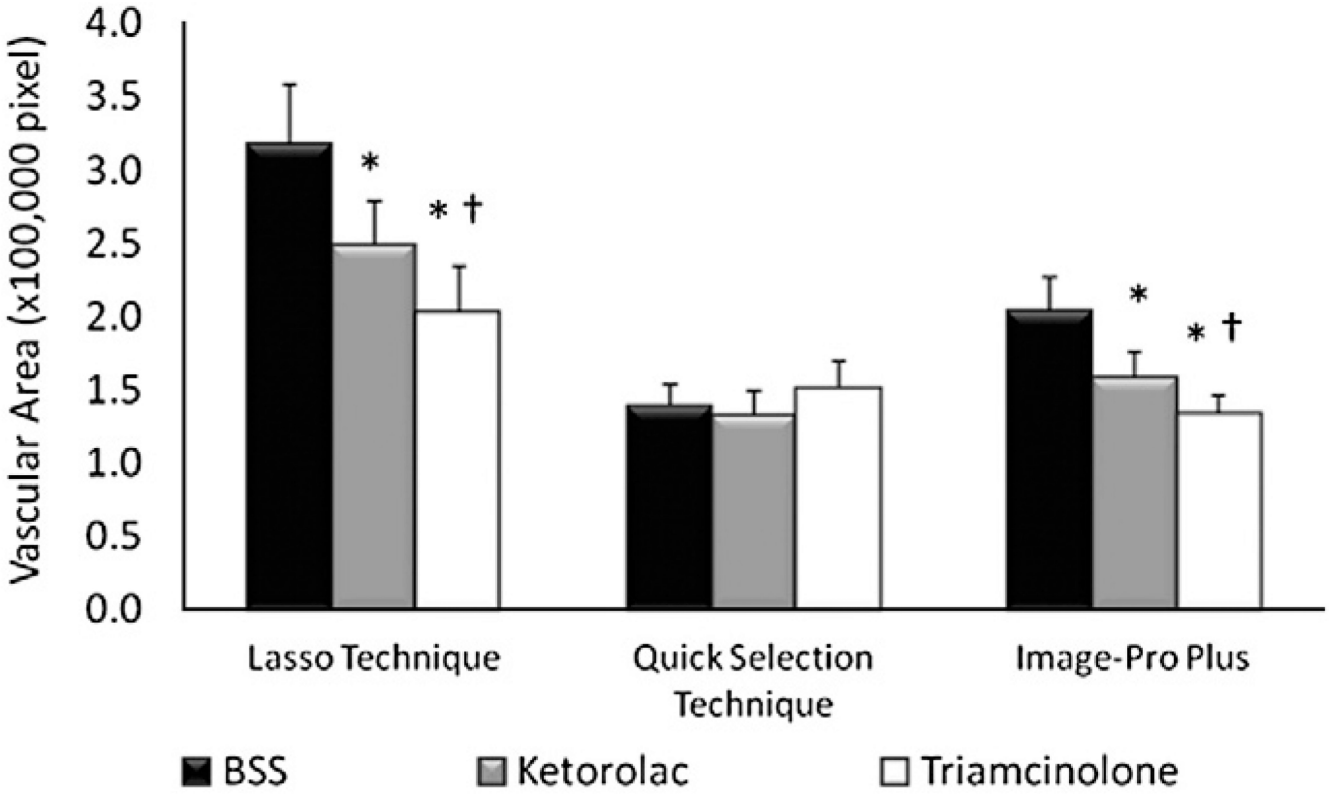

	Lasso Technique			Quick Selection Technique			Image-Pro Plus		
	BSS	Ketorolac	Triamcinolone	BSS	Ketorolac	Triamcinolone	BSS	Ketorolac	Triamcinolone
Mean Area (μm^2)	235	210	188	156	152	164	190	168	155
95% CI	14	12	13	9	10	10	10	9	8

Fig. 3.

CNV on choroidal mounts. Mean±95% confidence interval (CI) in pixels (upper graph) and calculated area in μm^2 (lower table) of vascular budding at 3 weeks after injection of BSS, ketorolac or triamcinolone injected eyes. * denotes statistically significant ($p<0.05$) difference between ketorolac and triamcinolone when compared to BSS. † denotes statistically significant ($p<0.05$) difference between ketorolac and triamcinolone.

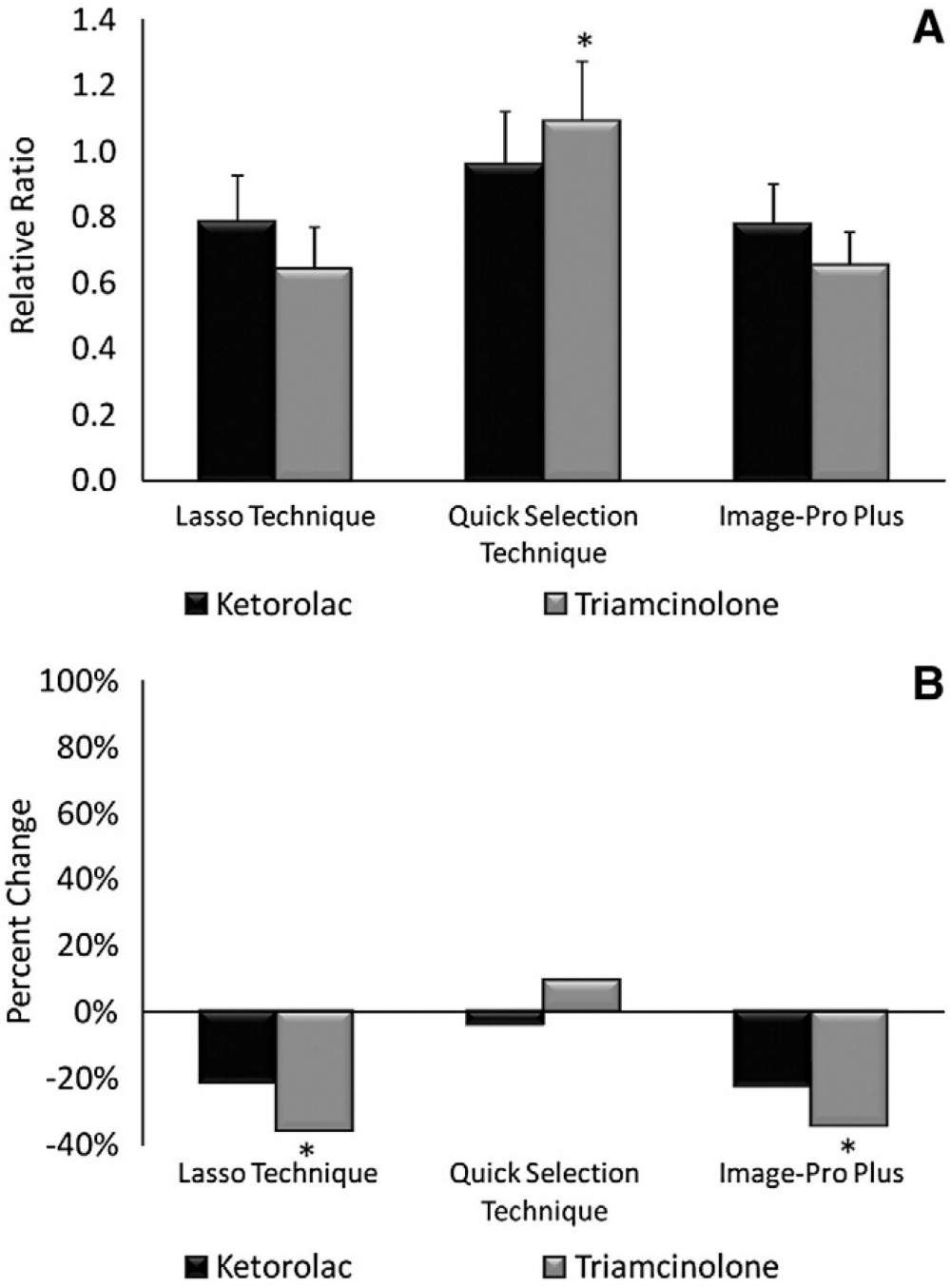

Fig. 4.

Relative ratio and percent change of CNV on choroidal mounts at 3 weeks. (A) Relative ratios ±95% CI of ketorolac and triamcinolone injected eyes. * denotes statistically significant ($p<0.05$) difference in triamcinolone for the Quick Selection Technique when compared to the Lasso technique or Image-Pro Plus. (B) Percent change of ketorolac and triamcinolone eyes. * denotes statistically significant ($p<0.05$) difference between ketorolac and triamcinolone.

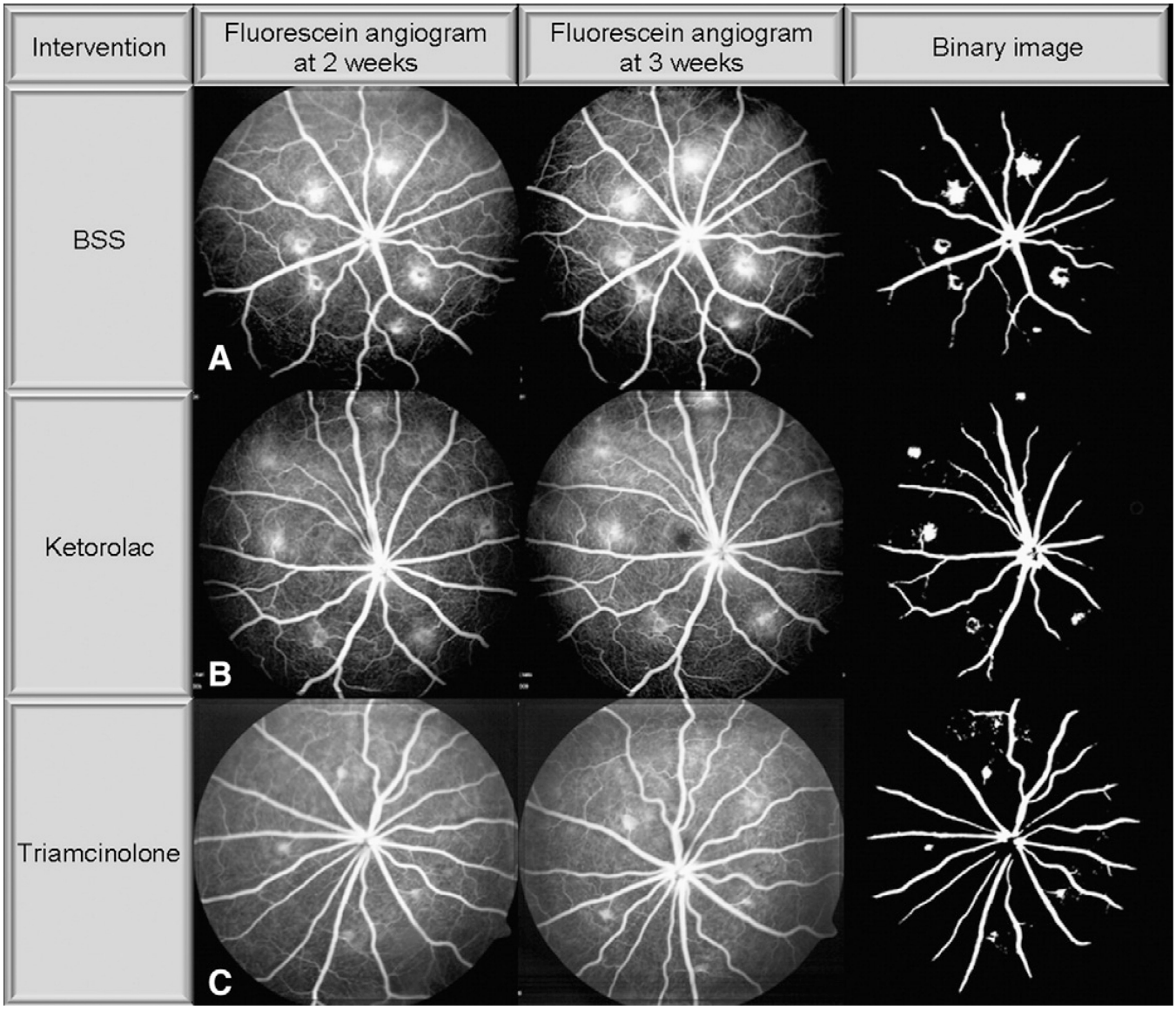

Fig. 5.

Laser-induced CNV on fluorescein angiogram. Representative images of CNV staining and leakage on fluorescein angiograms (FA) at 2 and 3 weeks after injection of (A) BSS, (B) ketorolac, or (C) triamcinolone. Note dramatically reduced staining and leakage in triamcinolone and to a lesser extent ketorolac injected eyes compared to BSS at 2 and 3 weeks.

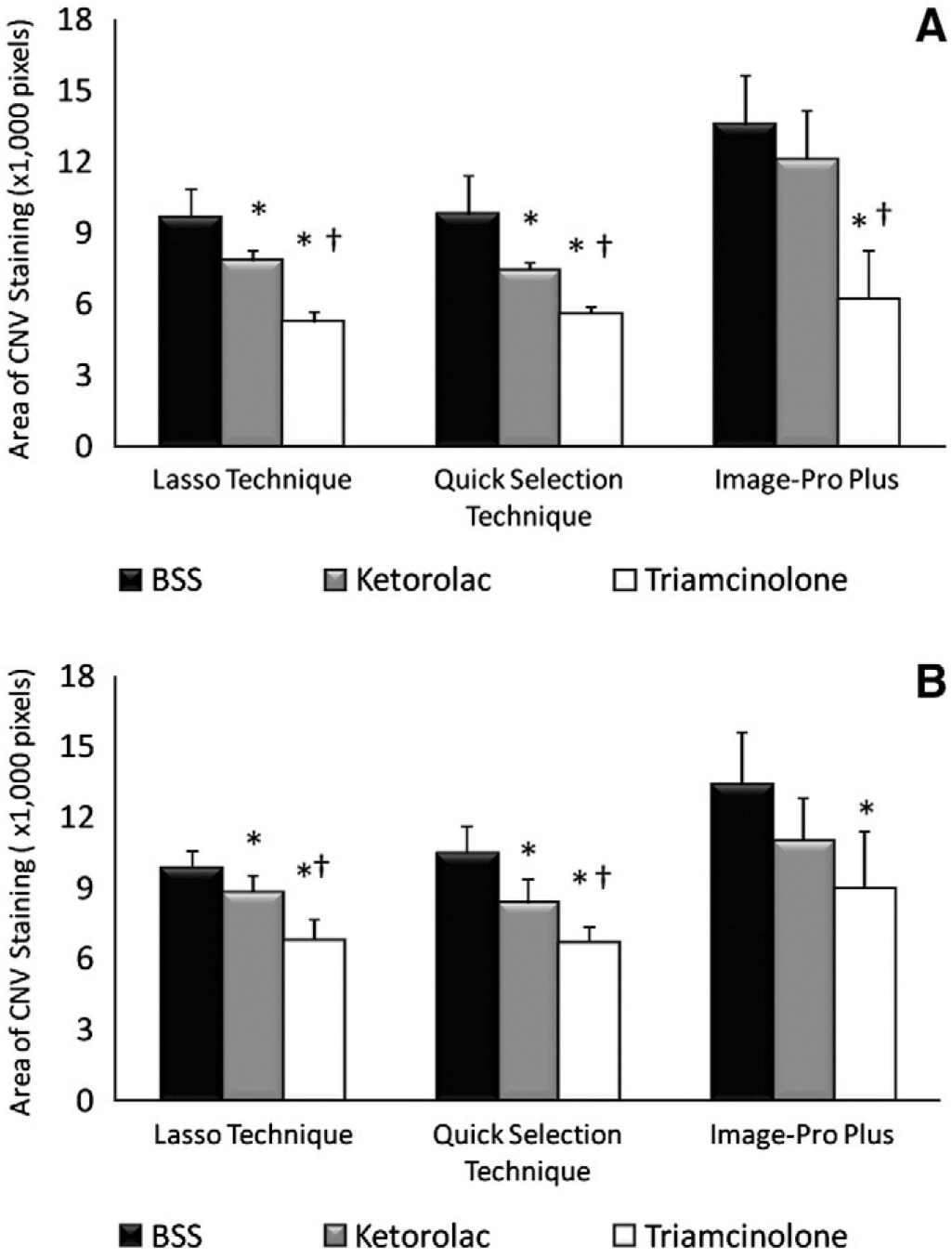

Fig. 6.

CNV on fluorescein angiogram. (A) Mean±95% CI CNV staining and leakage at 2 weeks after injection of BSS, ketorolac or triamcinolone. (B) Mean ± 95% CI CNV staining and leakage at 3 weeks after injection of BSS, ketorolac or triamcinolone. * denotes statistically significant (p<0.05) difference between ketorolac and triamcinolone when compared to BSS. † denotes statistically significant (p<0.05) difference between ketorolac and triamcinolone.

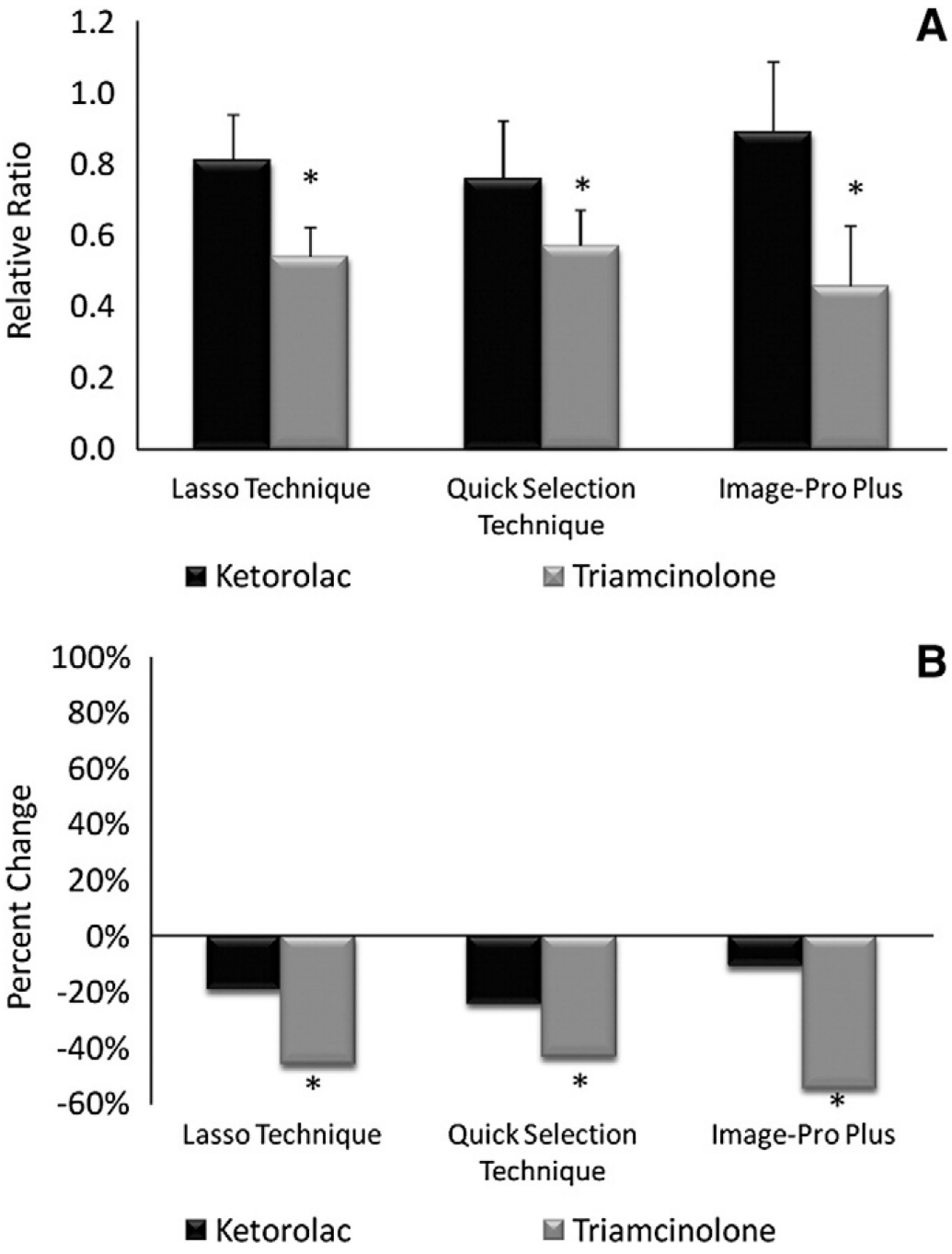

Fig. 7.

Relative ratio and percent change of CNV on fluorescein angiogram at 2 weeks. (A) Relative ratios ±95% CI of ketorolac and triamcinolone injected eyes. (B) Percent change in ketorolac and triamcinolone. * denotes statistically significant (p<0.05) difference between ketorolac and triamcinolone.

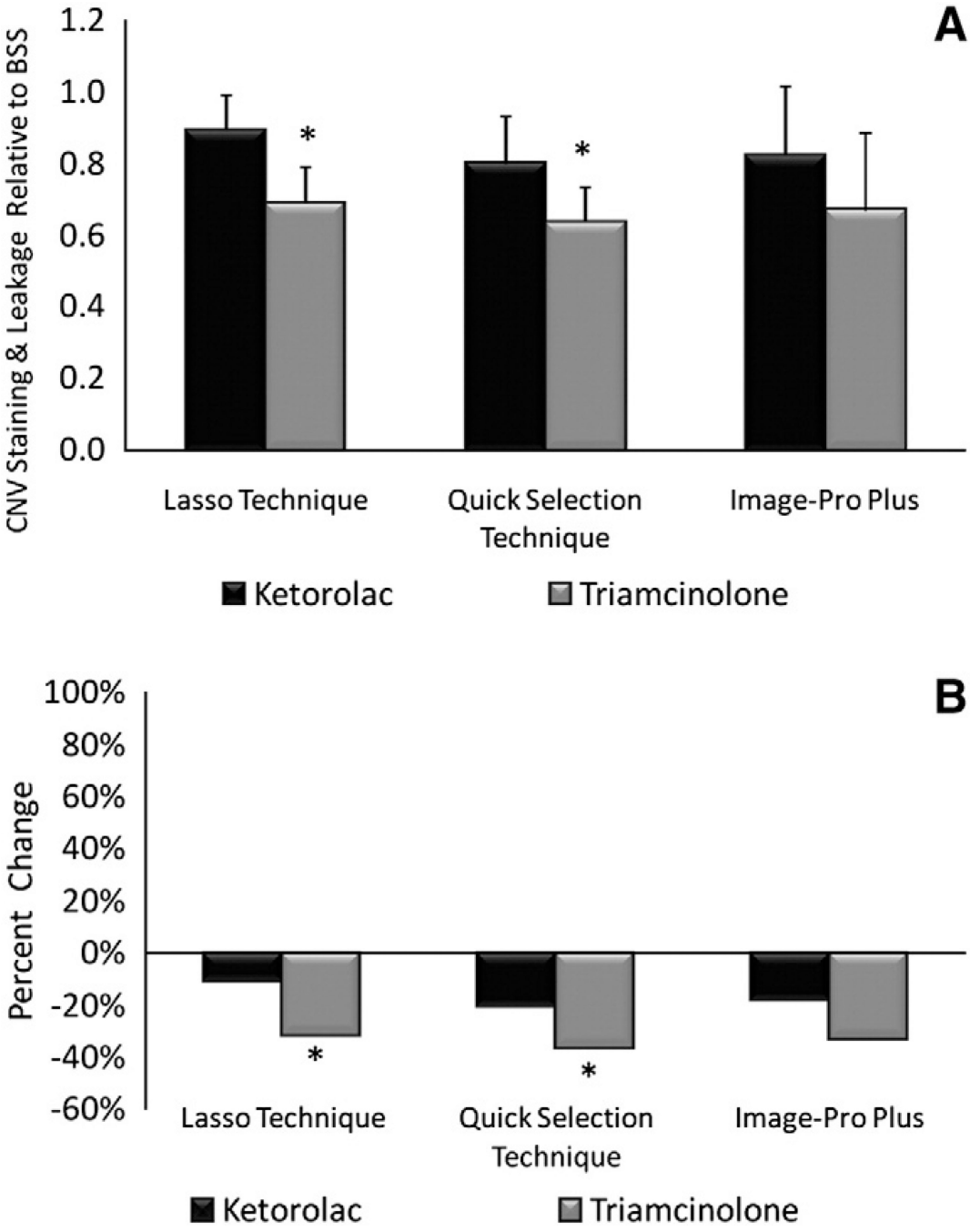

Fig. 8.

Relative Ratio and Percent Change of CNV on Fluorescein Angiogram at 3 weeks. (A) Relative ratios ±95% CI of ketorolac and triamcinolone injected eyes. (B) Percent change in ketorolac and triamcinolone. * denotes statistically significant (p<0.05) difference between ketorolac and triamcinolone.